journal

J. Am. Ceram. Soc., 89 [6] 1809–1815 (2006)
DOI: 10.1111/j.1551-2916.2006.01050.x


# Molecular Minerals™: Lyophillic Colloids for Ceramists

R. E. Riman† and G. A. Kumar

Department of Materials Science and Engineering, Rutgers, The State University of New Jersey, Piscataway, New Jersey 08854-8065

S. Banerjee and J. G. Brennan

Department of Chemistry and Chemical Biology, Rutgers, The State University of New Jersey, Piscataway, New Jersey 08854-8065

**This paper will focus on a novel class of inorganic compounds that we term as molecular minerals™ (MMs). MMs are clusters of ceramic fragments encapsulated with organic ligands. These compounds can be crystallized from solution as molecular single crystals and have well-defined crystal structures that can be described with X-ray diffraction methods. Most importantly, the ceramic clusters are perfectly monodisperse, and conventional synthetic techniques can be applied to facilitate control of size and composition. The organic encapsulate imparts solubility in organic solvents and polymers. More importantly, the solubility is thermodynamically driven to form a single-phase system. Thus, unlike nanoparticles, the stability of clusters in solution is spontaneous rather than kinetically derived. A critical tool for creating MMs is a firm understanding of the fundamental issues governing cluster structure and stability. We have demonstrated a unique synthetic approach to these materials, capable of creating materials with oxo, sulfido, selenido, or tellurido ligands, whose ceramic fragment size can currently be varied from about 0.5 to 2 nm. Both homometallic and heterometallic lanthanide (Ln) complexes incorporating the group 12 metals Zn, Cd, and Hg have been prepared. Relative to prior work on metal organic or organometallic Ln complexes, MMs have unprecedented luminescent properties in terms of emission wavelength, emission intensity, and quantum efficiency. These materials match or exceed the luminescent properties of ceramics, glasses, and nanomaterials, while having the additional advantage of polymer solubility. Solubility facilitates the preparation of transparent molecular mineral nanocomposites that can be fabricated as bulk polymers, fibers, and films.**

## I. Introduction

The heightened interest in nanomaterials processing has created a resurgence in colloidal processes utilizing nanopowders. Important technological barriers for single-phase and composite materials processing include control of the powder characteristics, suspension deagglomeration and stabilization, and particle manipulation, which all must be demonstrated on large length scales. This approach has the disadvantage that nanopowders and their dispersions are lyophobic colloids. By definition, they are energetically unstable because of their positive surface energy contribution of the solid–gas or solid–liquid interface. Thus, there is always a thermodynamic tendency to stabilize the system through energy minimization and flocculate the dispersed colloidal species. This paper will present a processing paradigm where energy minimization and uniform colloidal distribution are maintained.

Our processing paradigm utilizes lyophillic colloids. Lyophillic colloids form true solutions that form spontaneously through a strong interaction between the solvent and solute that minimizes the free energy.[1] Lyophillic colloids are typically based on organic constituents. Surfactant assemblies, biomolecules, and polymers are most commonly utilized in aqueous systems. However, a highly untapped resource for lyophillic colloids can come from the chemistry community, who are focused on the preparation of soluble inorganic cluster compounds that encompass a wide range of metal and non-metallic elements with a range of cluster sizes. Some of these clusters have thermodynamic stability, while others exist for kinetic reasons. Historically, inorganic clusters have been embraced by the materials community as precursors for synthesizing solid-state materials. Their structures have been designed to serve as stoichiometric building blocks for these materials via reactive pathways such as hydrolysis and polymerization.[2–6] A new promising research opportunity is to use these compounds for their intrinsic materials properties rather than as precursors. For the sake of practical utility, these compounds must not only be soluble in solution but must also possess no driving force to react. Thus, this paper will present a new family of cluster compounds whose stability is thermodynamically driven and whose properties can match or even exceed those of the materials they are targeted to emulate.

A range of enabling property opportunities can be identified for electronic, optic, magnetic, and multifunctional applications. This paper will consider lanthanide (Ln) materials as a platform to exploit this opportunity afforded by cluster chemistry. Lns rely on radiative electronic transitions utilizing their 4f-electrons. Unfortunately, conventional Ln cluster compounds typically contain organometallic and metal–hydroxide bonds whose phonon energies are sufficiently high to quench these transitions non-radiatively (vibronically) to reduce quantum efficiency, typically to less than 1%.[7–11] Significantly higher quantum efficiency can be easily achieved with conventional ceramic crystals or glasses as they can be processed to avoid these types of structural features. However, ceramics cannot be dissolved into conventional solvents or polymers without decomposition. Thus, the paradigm lyophillic colloidal system must consist of molecular species that combine the structural features that are found in conventional ceramics with the solubility behavior typically found for molecular compounds.

## II. Molecular Minerals™

Cluster compounds that address the needs of the paradigm system are termed Molecular Minerals™ (MMs). MMs consist of an inorganic core and a covalently tethered organic encapsulant as shown in Fig. 1. The organic encapsulant is ligated to the inorganic core in a structured fashion, with both ionic ($EPh^-$)

G. Messing—contributing editor

Manuscript No. 21352. Received January 8, 2006; approved February 24, 2006.
Presented at the 9th International Ceramic Processing Science Symposium, Coral Springs, FL, January 8–11, 2006.
This work was supported by National Science Foundation (CHE 0303075), New Jersey State Commission on Science and Technology, USR Optonix, and the U.S. Army.
†Author to whom correspondence should be addressed. e-mail: riman@email.rci.rutgers.edu

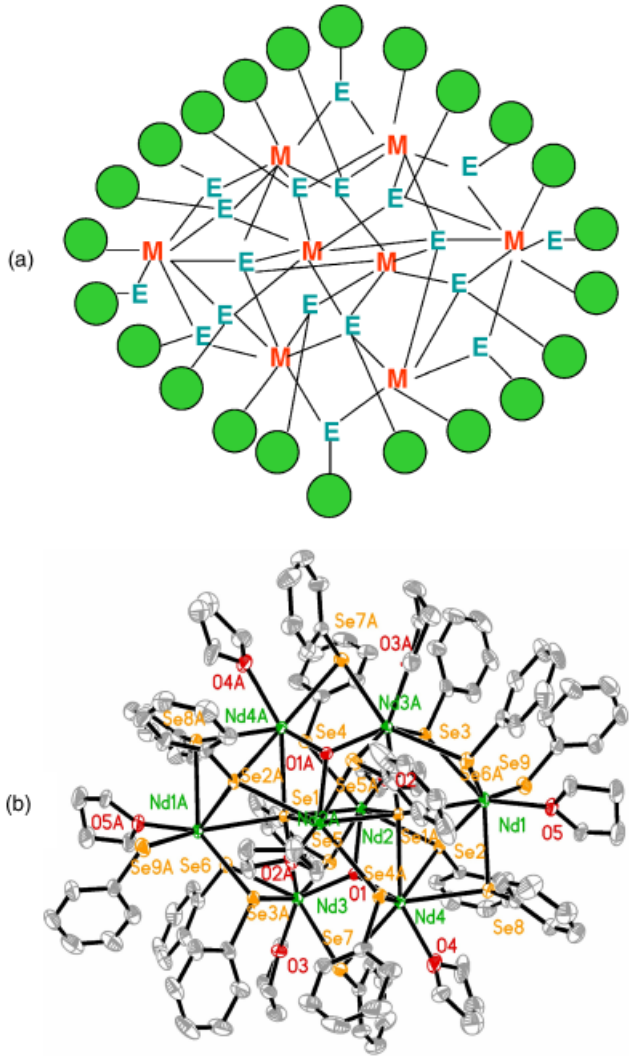


**Fig. 1.** (a) Structure cartoon of the Molecular Mineral™ concept and (b) molecular structure of $Nd_8O_2Se_2(SePh)_{16}$.

and dative ($NR_3$, $OR_2$) components. MMs are typically neutral in charge and can be precipitated as single-phase systems directly from solution by regulating the solvency of the molecular species. The molecular species that comprise the unit cell consist of one or more units. MMs can be readily recovered in single-crystal form (Fig. 2) enabling precise structural determination of the inorganic and organic components of the cluster. As the cluster is encapsulated with organic ligands, solvency in both polar and non-polar media is possible. Figure 2 shows a photograph of a transparent and hence uniform non-aqueous solution of MMs. Paradigm MMs dissolve as the molecular building blocks that make up the unit cell of a single crystal. MMs readily dissolve in both conventional solvents such as tetrahydrofuran (THF) and pyridine or in polymers such as perfluorcyclobutyl (PFCB) 6F variants.[12] The solubility of MMs in various media facilitate the use of well-established polymer processing techniques for device fabrication. This advantage opens up a range of materials integration opportunities that would be not possible if high-temperature ceramic processing was necessary.

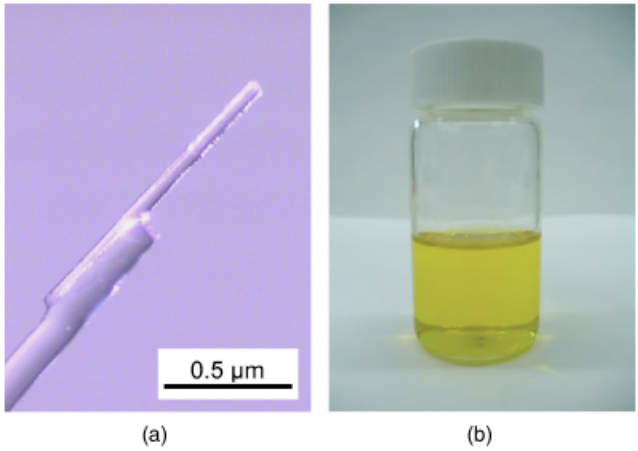


**Fig. 2.** (a) $(THF)_3Er(SePh)_3$ Molecular Mineral™ (MM) single crystal and (b) 0.06*M* $(THF)_3Er(SePh)_3$ MM solution.

**Table I. Summary of Reported Lanthanide Clusters**

| Cluster | Ln | References |
|---|---|---|
| $(py)_6Ln_2(Se_2)(Se)Br_2$ | Ho, Er, Yb | Huebner *et al.*[16] |
| $(py)_8Ln_4Se_4(SePh)_4$ | Yb | Freedman *et al.*[26] |
| $[(THF)_8Ln_4Se(SePh)_8]^{2+}$ | Nd, Sm | Freedman *et al.*[17] |
| $(py)_8Ln_8Se_6(SePh)_{12}$ | Nd, Sm | Freedman *et al.*[24,28] |
| $(THF)_8Ln_8S_6(SPh)_{12}$ | Ce, Pr, Nd, Sm, Gd, Tb, Dy, Ho, Er | Melman *et al.*[25,27] |
| $(py)_8Ln_8S_6(SPh)_{12}$ | Nd, Sm, Er | Melman *et al.*[25] |
| $(THF)_6Ln_4E_9(SC_6F_5)_2$ | Tm, Yb | Fitzgerald *et al.*[18] |
| $(py)_9Ln_4Te_9TePh_2$ | Sm, Tb, Ho, Tm | Freedman *et al.*[19] |
| $(THF)_6Ln_4I_2(SeSe)_4(\mu_4\text{-}Se)$ | Tm, Ho, Er, Tb | Kornienko *et al.*[20] |
| $(THF)_{10}Ln_4I_6Se_6$ | Yb | Kornienko *et al.*[20] |
| $(py)_8Ln_4Se_9(EPh)_2$ | Yb | Kornienko *et al.*[21] |
| $(DME)_4Ln_4Se(SePh)_8$ | Nd/Sm(III); Sm/Yb(II) | Freedman *et al.*[22] |
| $(THF)_6Ln_4I_2S_9$ | Er, Tm, Yb | Melman *et al.*[23] |
| $(py)_8Ln_4M_2Se_6(SePh)_4$ | Er, Yb, Lu | Kornienko *et al.*[15] |
| $(THF)_{10}Ln_6S_6I_6$ | Er | Kornienko *et al.*[13] |
| $[(DME)_7Ln_7S_7(SePh)_6]^+$ | Nd | Freedman *et al.*[28] |
| $(py)_{10}Ln_6S_6(SPh)_6$ | Yb | Freedman *et al.*[26] |
| $(THF)_8Ln_8O_2Se_2(SePh)_{16}$ | Ce, Pr, Nd, Sm | Banerjee *et al.*[14] |
| $(THF)_{14}Ln_{10}S_6(Se_2)_6I_6$ | Dy, Ho, Er | Kornienko *et al.*,[13] Huebner *et al.*[16] |

We have prepared a wide range of Ln MMs, as summarized in Table I.[13–28] We have focused on non-oxide Ln compounds because of their appealing optical and semiconductor properties. However, a much broader range of compounds are possible that can encompass a wide range of active and passive properties. Our synthesis approach involves a room-temperature 1- or 2-pot solvothermal process.[24,25,27] A typical reaction scheme for a monometallic cluster is shown below:

$$8\,\mathrm{Ln} + 12\,\mathrm{PhE-EPh} \xrightarrow{\text{solvent}} 8\,\mathrm{Ln(EPh)_3}$$
$$\times \xrightarrow{\mathrm{E}} (\text{solvent})_8\mathrm{Ln_8E_6(EPh)_{12}} + 6\,\mathrm{PhEEPh}$$

where Ln = Ce, Pr, Nd, Sm, Gd, Tb, Dy, Ho, Er; E = S, Se; and Ph = $C_6H_5$.

Thus, MMs can be prepared with conventional chemical manufacturing methods. In our early work, many of our compounds were found to be highly air sensitive. However, recent developments have focused on the introduction of fluorinated ligand systems that are considerably more tolerant of atmospheric conditions, to the point that some can be handled in air.[13]

Single-crystal X-ray methods demonstrate that the various compounds shown in Table I are monodisperse clusters. The ceramic cores of these clusters range from 0.5 to 2 nm. A variety of cluster structures and compositions have been demonstrated for monometallic and bimetallic complexes. The monometallic or bimetallic building blocks that make up the unit cells com-

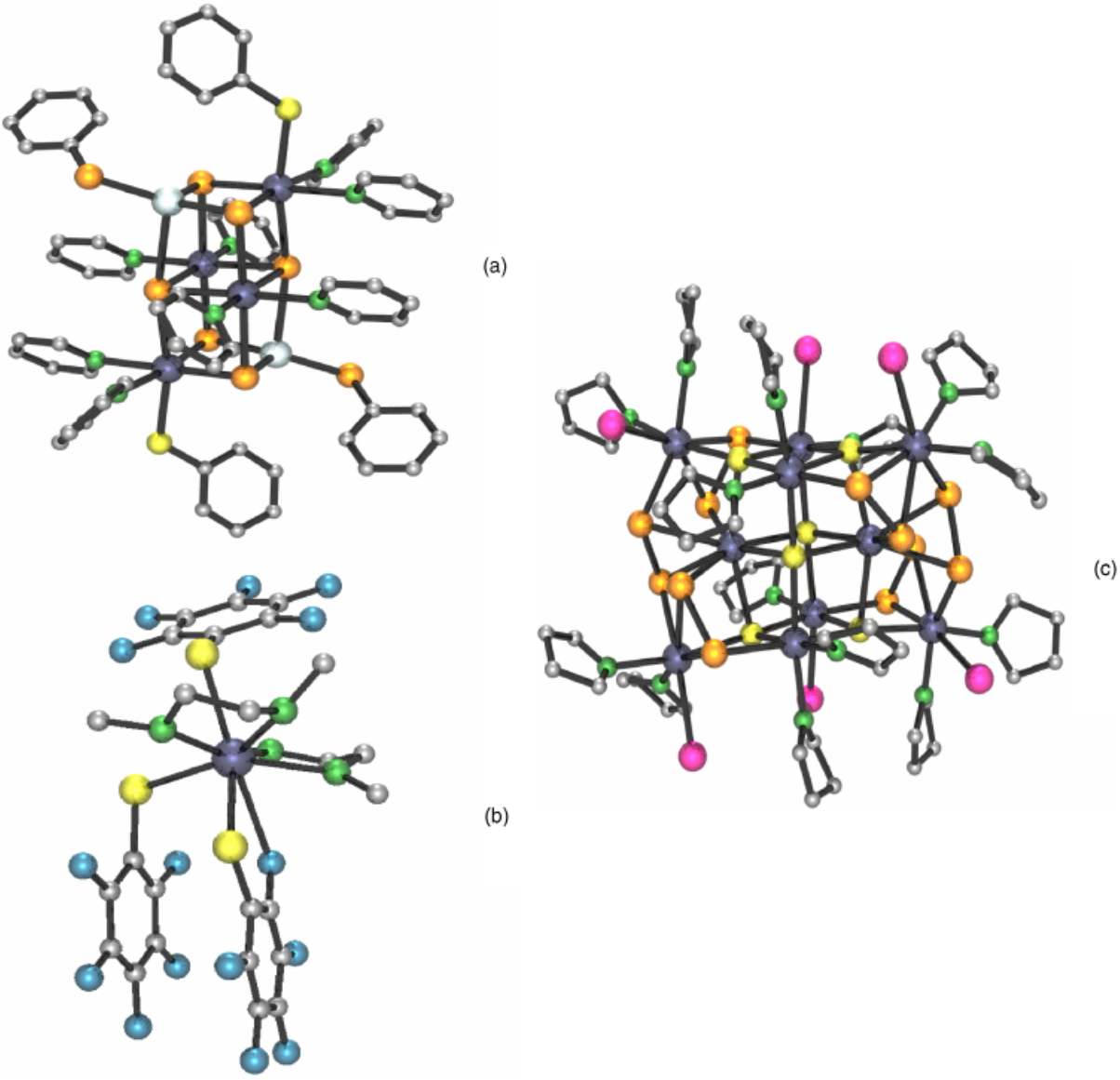


**Fig. 3.** Molecular Minerals™ with different types of coordination environments with orange Se, yellow S, gray Ln, white M, blue F, pink I, and green Lewis base (O, N) atoms: (a) $(py)_8Er_4M_2Se_6(SePh)_4$[M = Hg,Cd] (b) $(DME)_2Er(SC_6F_5)_3$ (c) $(THF)_{14}Er_{10}S_6(SeSe)_6I_6$ is a hierarchic encapsulate of an S coordination sphere, followed by a coordination sphere of Se.

prise anywhere from 1 to 8 molecular units, and each molecular unit has from 1 to 10 metal cations. Figure 3 shows the wide range of ligand environments, where ligands can be disordered, ordered, and hierarchic. A similar type of control should also be possible as further control is gained over the placement of metals in these compounds. For example, in the recently described oxo clusters $(THF)_8Ln_8O_2Se_2(SePh)_{12}$, there are two well-defined Ln coordination environments: those with Ln coordinating the oxo ligands and those that do not.[14] We have found that it is possible to prepare hetero-Ln clusters with this formulation, in which we can control the occupancy of the non-oxo site. This type of control of the coordination environment is not possible with the solid solutions or glasses used for conventional ceramic Ln hosts (e.g., selenide, sulfide).[29] As the distributions of species such as chalcogenides or halide species are disordered, this advantage provides a highly controlled way to introduce both cations and anions as a means to fine tune electronic band structure, polarity, and many other fundamental properties that control electronic, optical, and magnetic properties.

## III. Luminescent MMs

There is tremendous interest in Ln-containing ceramic materials as luminescent materials for light amplification, displays, taggants, and lasers.[30–34] Brightly emitting materials require that all of the 4f electrons used for a specific electronic transition yield photons instead of phonons (lattice vibrations). Further, the Ln concentrations in the lattice must be as high as possible. For efficient emission of light, a host lattice must be chosen that has low phonon energy. Low phonon energy hosts are increasingly more important for high quantum efficiency emission as the emission wavelength becomes longer. In general, Ln materials consisting of weakly bonded heavy anions such as chloride, fluoride, sulfide, and selenide have suitably low phonon energies.[35] This low phonon energy concept has been demonstrated with MMs using erbium as a Ln ion. Figure 4 shows absorption and corresponding emission spectra for two erbium-containing MM complexes where Er1 and Er10 are $(DME)_2Er(SC_6F_5)_3$ and $(THF)_{14}Er_{10}S_6Se_{12}I_6$, respectively. The quantum efficiencies for these complexes are in the range of 75%–78%, which are the highest reported values to date for molecular compounds.[13]

These emission properties are comparable with what has been observed for erbium-doped low phonon energy ceramic hosts.[36–40] Figure 5 shows emission data for erbium MMs and erbium-doped single crystals, glasses, and nanocrystals. Table II summarizes a comparison of the emission spectral properties of MMs with a representative group of well-known low phonon energy hosts. These data show that the quantum efficiencies for

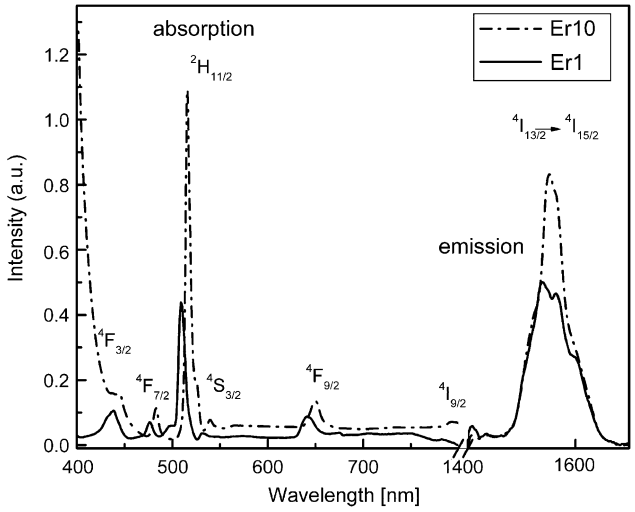


**Fig. 4.** Comparison of the optical absorption and emission spectra of Er1 and Er10 Molecular Minerals™ with the standard spectroscopic notation for observed transitions.

all of these materials are similar with MMs having a lower efficiency but again, a much higher value than observed with previously published molecular compounds. These results suggest that the molecular building blocks found in the as-precipitated single crystals are maintained when these molecular crystals are dissolved. In the systematic preparation of emissive MMs, the critical structural features to avoid are direct bonds between Ln and anions with CH, NH, or OH functionalities, as these species have high phonon energies. This is best illustrated with the work we have performed on the $(DME)_2Er(SC_6F_5)_3$ monomer where quantum efficiencies as high as 75% have been observed.

Our work on these Ln complexes suggests for the most part that the precipitated crystals dissolve into the solution as molecular clusters. Both absorption and emission spectra of the single crystals match those of the crystals dissolved in solution, whether the solution is a conventional solvent like THF or PFCB polymers. However, differences have been observed that suggest that a more complex solution phenomenon is ongoing for some of our clusters. For example, $(THF)_{14}Er_{10}S_6(SeSe)_6)I_6$ (Er10) and $(DME)_2Er(SC_6F_5)_3$ (Er1) have quantum efficiencies of 78% and 75%, respectively, when characterized in THF and DME solvents. However, when these compounds are compared in PFCB polymers, differences in the emission spectral properties were observed. Our studies on various polymers show subtle

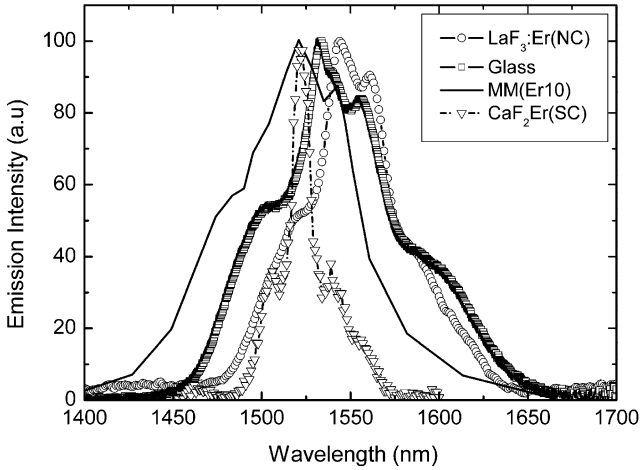


**Fig. 5.** Comparison of the infrared emission spectrum of Er10 Molecular Minerals™ with erbium-doped systems incorporating the following hosts: single crystals of $CaF_2$, nanocrystals of $LaF_3$, and a telluride glass.

**Table II. Comparison of the Infrared Fluorescence Spectral Properties of Er10 with Other Solid-State Hosts**

| Host | Wavelength (nm) | Emission cross section ($10^{-20}$ cm$^2$) | Lifetime (ms) | Quantum efficiency (%) |
|---|---|---|---|---|
| Er10 | 1542 | 1.4 | 3 | 78 |
| Tellurite Glass[36] | 1534 | 0.82 | 4.0 | 100 |
| $LaF_3$:Er(NC)[39] | 1540 | 0.33 | 10.9 | 100 |
| $CaF_2$:Er(SC)[40] | 1530 | 3.2 | 8.5 | 100 |

spectral differences, which suggest that the solvent environment may be modifying the complex via inhomogeneous broadening (Fig. 6), most likely by displacement of the dative Ln–O interactions with Ln–polymer interactions. More research detailing the physical chemistry of MM solutions is needed to detail how MMs interact with solvents and polymers and whether or not there are any chemical reactions taking place.

Ln species are typically dissolved into ceramic lattices or glass networks (conventional solid-state materials) where the Lns randomly substitute for other cation species (e.g., Er substitutes for Te in tellurite glass).[36] This random substitution leads to clustering of Lns. When the Ln spacing is too close in such lattice clusters, Lns can interact to quench the excited f electrons non-radiatively, which results in concentration quenching. The phenomenon of concentration quenching occurs through multi-polar interaction between ion pairs. Concentration quenching occurs by matching energy levels of neighboring Lns, as described by the Forster–Dexter theory.[41,42] According to this theory, the probability of this non-radiative quenching interaction is inversely proportional to the $n$th power of the Ln–Ln separation distance of a selected rare-earth pair under consideration (where, $n = 6$, 8, and 10). The $n$th power for the interaction depends on the dominant concentration quenching mechanism, which could be one or more of the following: dipole–dipole, dipole-–uadrupole, and quadrupole–quadrupole. In Er10, the major contribution to concentration quenching comes from the dipole–dipole interaction where $n = 6$ and the electron transition rate varies inversely with the square of the ionic concentration.[43] Generally, in Ln-doped crystalline materials, it is customary to define the term critical separation, $R_o$, at which the energy transfer rate approaches the decay rate. The decay rate consists of radiative and non-radiative terms. At this separation distance or greater, the decay rate of a specific electronic transition can be purely radiative. However, at shorter distances, the radiative

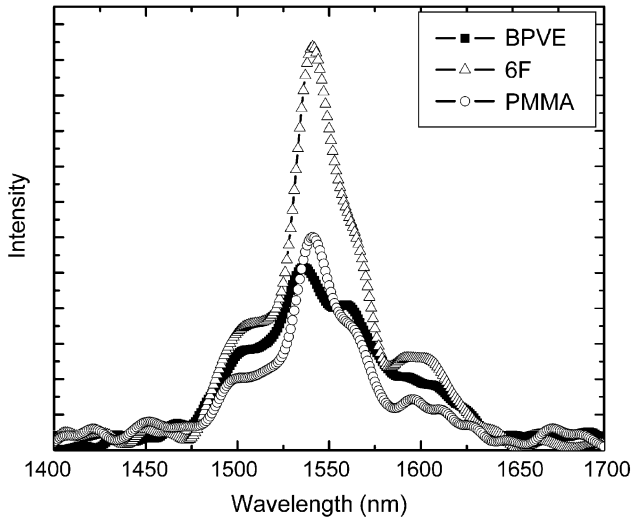


**Fig. 6.** Infrared emission spectra of Er1 Molecular Minerals™ in the polymers perfluorcyclobutyl (PFCB) (6F), PFCB (BPVE), and PMMA. Er1 concentration in each polymer is 0.023 mmol Er1/g polymer.

decay rate decreases and concentration quenching can begin to reduce quantum efficiency. Typically for rare-earth-doped crystals, the critical separation is ~2–2.5 nm, which corresponds to an ionic concentration of $10^{20}$ ions/cc. However, in a complex crystalline structure like that of Er10, in addition to ion pair separation, both the molecular structure and symmetry are also important considerations for computing the contribution of concentration quenching toward reducing quantum efficiency. Those that are below the critical separation will reduce quantum efficiency in an increasingly non-linear manner, which requires a detailed analysis for proper assessment.

Our work with Er10 has led to concentrations as high as $3.3 \times 10^{21}$ ions/cc in the pure crystals that still achieve quantum efficiencies as high as 78%. This crystalline nature of MMs could provide a scientific platform for understanding the emission characteristics of conventional crystalline or amorphous inorganic materials and how clustering of ions in these networks influences phenomena such as concentration quenching. We believe that the knowledge of the rare-earth spacing, structure, and symmetry of these molecules offer well-defined, narrowly distributed rare-earth environments enabling the development of emission models and the definition of optical and structural parameters that can only be estimated in conventional crystalline and amorphous materials. The influence of structure and symmetry is evident indirectly by examining the average intermolecular and intramolecular Ln spacings. First, consider the intermolecular Ln spacing. The organic ligands encapsulating the Lns pose a spacing of about 1 nm, which, in a conventional solid-state material, would normally be interacting. Because of this spacing, MMs can be dissolved in solution up to their solubility limit without any evidence of concentration quenching. Thus, instead of reaching a maximum in emission intensity as a function of Ln concentration, the intensity can be observed to increase with increasing concentration. This is demonstrated in Fig. 7 for the Er1 complex dissolved in DME where emission peak area (also intensity) increases with increasing Er1 concentration. However, the increase in peak width with Er1 concentration also demonstrates that inhomogeneous broadening is also taking place, which means that emission-related interactions are occurring between Er1 molecules or between Er1 molecules and the solvent. Second, consider lattice site spacing within the inorganic core. In Er10, the two shortest separation distances between two Er atoms are 0.39 and 1.025 nm. Both the intermolecular and intramolecular distances observed in MMs are shorter than typical 2–2.5 nm distances observed in solid-state materials.

Monte-Carlo energy transfer modeling simulations[43] for Er10 have suggested that concentration quenching is the primary mechanism responsible for reduction of quantum efficiency.

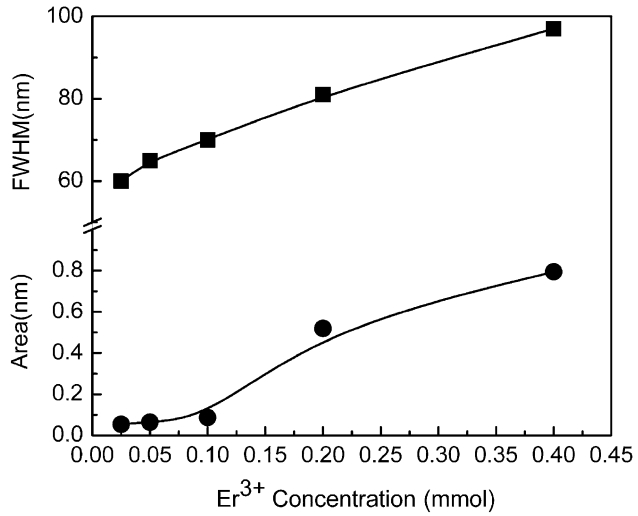


**Fig. 7.** Concentration dependence (millimoles) of emission bandwidth and area in $(DME)_2Er(SC_6F_5)_3$ in 5 mL of DME.

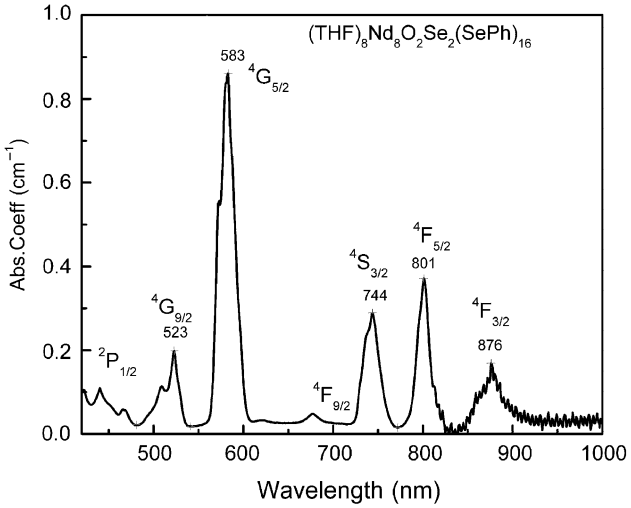


**Fig. 8.** Absorption spectrum of 0.0046*M* $(THF)_8Nd_8O_2Se_2(SePh)_{16}$ in tetrahydrofuran (THF) with spectroscopic notation for the observed band transitions. Adapted with permission from Reference 14. Copyright 2005 American Chemical Society.

The critical separation distance, $R_o$, for the Er10 MM is about 1.5 nm, which is larger than the typical interionic distances observed in MMs. The computations also suggest that if we can increase the smaller separation distances from 0.39 nm to some higher value, an opportunity exists to design new MMs that exhibit quantum efficiencies approaching 100% while maintaining a high Ln concentration.

An alternative way to improve emission intensity is to utilize this energy transfer interaction by supplying an appropriate Ln co-dopant with the primary Ln ion responsible for emission. Enhanced emission intensity is accomplished by non-radiative energy transfer from the co-dopant to the primary ion. Yb is a common co-dopant for enhancing Er emission in this fashion. Work is in progress to attempt to further improve emission in this fashion. Thus, so far, we have demonstrated the capability to make heterometallic complexes containing Hg and Cd with Lns of Yb, Er, or Lu. Our future work is seeking to use this heterometallic approach where Yb substitutes for the Hg or Cd.

Molecular complexes containing 1, 7, and 8 Nd atoms at various lattice locations have been recently synthesized and their optical properties were studied. As trivalent Nd is the most efficient ion for laser applications in various hosts, our interest was to study the spectroscopy of this new class of MMs. Our attention was turned to $(THF)_8Nd_8O_2Se_2(SePh)_{16}$ (Nd8) and $(DME)_2Nd(SC_6F_5)_3$. (Nd1). A typical absorption and emission spectra of the $(THF)_8Nd_8O_2Se_2(SePh)_{16}$ complex is shown in Figs. 8 and 9. Both the absorption and emission spectra are similar to the solid-state materials in terms of the spectral intensity, width, and Stark splitting (a multiple division of the spectral band because of the electrostatic field from surrounding ligands). One unexpected result is an emission band at 1850 nm. This band has never been observed in a high phonon energy host like an oxide but has been observed in Nd-doped ZBLAN glass.[44] We attribute this observation to the low phonon energy coordination environment for the Nd, which prevents the non-radiative decay of the 1850 nm band. Fluorescence quantum efficiencies of 16% and 9% are obtained for the 1060 nm emission for Nd8 and Nd1, respectively. These values are the highest reported efficiencies for molecular Nd compounds. Earlier, Hasegawa *et al.* [11] obtained a decay time of 13 μs and a quantum efficiency of 3.2% for Nd (bis-perfluorooctanesulfonylimide)$_3$. Other workers report quantum efficiencies in the range of 0.001% to 1%.[7,45–49]

Our spectroscopy work on various Er- and Nd-doped MMs has given us an opportunity to evaluate these materials as candidates for important photonic applications such as low-power lasers and active fibers and waveguides. A summary of the optical properties of the Nd complexes is given in Table III in

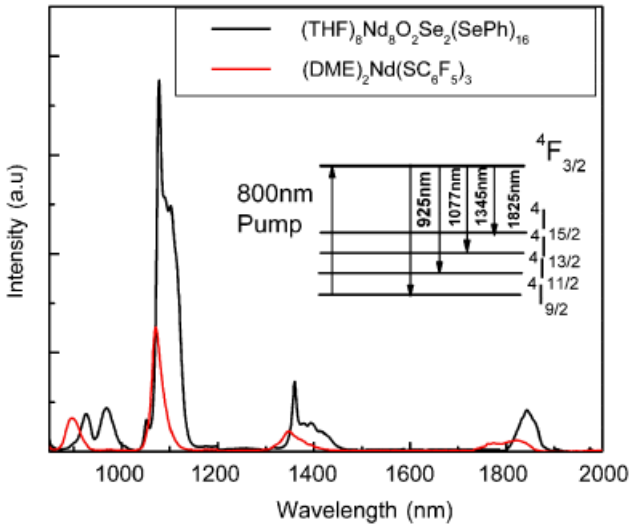


**Fig. 9.** Comparison of the emission spectra of $Nd^{3+}$ for Nd8 and Nd1 Molecular Minerals™. Pumping scheme and emission channels are shown in the inset. Adapted with permission from Reference 14. Copyright 2005 American Chemical Society.

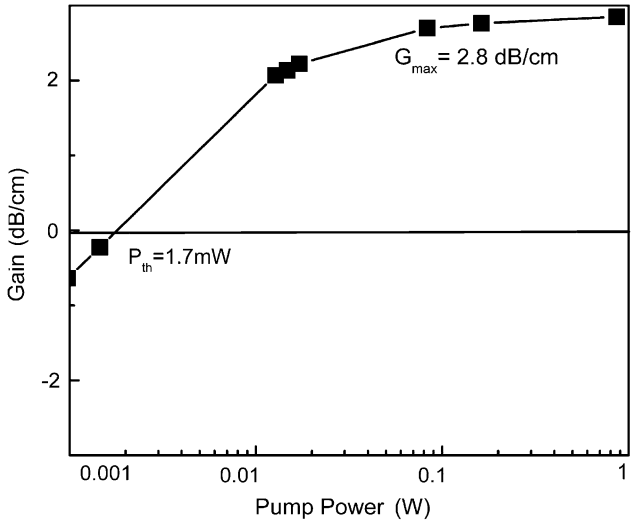


**Fig. 10.** Simulated optical gain as a function of the pump power in the $(THF)_{14}Er_{10}S_6Se_{12}I_6$/6F nanocomposite planar wave guide structure. Reprinted with permission from G. A. Kumar et al., *Appl. Phys. Lett.* 2006, 88, 091902/1-091902/3. Copyright 2006, American Institute of Physics.

comparison with the well-known laser host Nd:YAG.[50] The stimulated emission cross-section, $\sigma_e$, is an important optical parameter that defines the optical gain of the amplifier system. $\sigma_e$ is more than seven times higher in Nd:YAG compared with Nd8. However, both Nd8 and Nd1 have significantly higher Ln concentrations, which are as much as $\sim$14 times higher than Nd:YAG ($19 \times 10^{20}$ ions/cc in Nd8, $13 \times 10^{20}$ ions/cc in Nd1, and $1.4 \times 10^{20}$ ions/cc in Nd:YAG). Thus, the lower $\sigma_e$ values for MMs are amply compensated by their higher Ln concentrations, enabling them to be suitable candidates for laser and amplifier applications in bulk, fiber, or thin-film form. Moreover, these devices can be processed with low-temperature solutions instead of the high-temperature processes needed for materials such as YAG.

For Er1 MMs, we are in the process of fabricating planar wave-guide structures capable of optical amplification at 1550 nm. Using the measured values of the optical parameters for the Er complexes, an estimate can be made for the optical gain and threshold pump power for a planar wave-guide amplifier.[51] Our numerical simulation utilized a planar film $2 \times 1$ $\mu m^2$ geometry for either an Er10/6F or Er1/6F nanocomposite. The predicted optical gain characteristics of Er10/6F composite wave guide are shown in Fig. 10. The maximum gain obtained for Er10 and Er1 is 2.8 and 0.021 dB/cm, respectively, with a corresponding threshold pump power of 1.7 and 0.2 mW. These threshold values are many times smaller than other reported Er-based organic complexes, which are of the order of 900 mW because of the very low fluorescence decay time of the 1550 nm band. It should be noted that this threshold power is comparable with the 1.4 mW reported for Er–polydendate cage complexes wherein the pumping is carried out through the aromatic ligand at 287 nm[52] and also to 1.5 mW reported for inorganic systems like Er-doped silicate or Er-doped $Al_2O_3$ waveguides[53] and Er-doped $CaF_2$:Er/6F PFCB fluoropolymer nanocomposite.[54] The low optical gain in Er1/6F is due to the comparatively lower Er concentration relative to Er10/6F. The low pump threshold and high gain are potentially useful for the application of optical amplifiers. Addition of $Yb^{3+}$ in selected lattice positions of Er10 may further increase the optical gain, and experiments are underway to investigate this possibility.

**Table III. Fluorescence Spectral Properties of Nd1, Nd8 Clusters, and Nd:YAG Single Crystals**

| Transition from $^4F_{3/2}$ to | Wavelength (nm) | $\beta_{ex}$† (%) | $\tau_{fl}$(μs)‡ | | | $\sigma_e(10^{-20}$ cm$^2$)§ | | |
|---|---|---|---|---|---|---|---|---|
| | | | Nd8 | Nd1 | YAG | Nd8 | Nd1 | YAG |
| $^4I_{15/2}$ | 1843 | 9 | 186 | 111 | 259 | 0.0138 | 0.0092 | – |
| $^4I_{13/2}$ | 1360 | 14 | | | | 0.29 | 0.30 | 6.0 |
| $^4I_{11/2}$ | 1078 | 72 | | | | 3.04 | 1.61 | 22.0 |
| $^4I_{9/2}$ | 927 | 6 | | | | 1.72 | 0.71 | 4.0 |

†Measured fluorescence branching ratio. ‡Fluorescence decay time. §Stimulated emission cross section.

## IV. Summary

MMs are lyophillic colloids that provide a novel means to process nanomaterials without the agglomeration/aggregation and colloidal stability issues associated with lyophobic colloids. MMs can be prepared for a wide range of Lns and with a wide range of structures for a given Ln. Low-temperature solvothermal approaches have been developed that enable preparation of MMs that offer a low phonon energy environment for the Ln. Luminescent materials result that exhibit highly efficient emissions as well as novel emission wavelengths. In addition, the unique crystalline structures offered by MMs also provide unprecedented high concentrations of Lns that further contribute toward intensifying light emission. Data analysis of the optical properties reveals promising device opportunities, which include lasers and optical amplifiers, among many other applications, that can exploit the advantages of highly emissive materials. The ability to synthesize these materials with solvothermal methods and process these materials with polymer processing methods make these materials commercially appealing.

## Acknowledgments

The authors would like to acknowledge Tetramer Technologies, LLC (Earl Wagener, Shengrong Chen), for the generous supply of PFCB fluoropolymers and helpful advice in processing these polymers.

## References

[1]R. Hunter, *Foundations of Colloid Science*, p. 5 Oxford University Press, Oxford, 2001.
[2]Y. Suwa, Y. Sugimoto, and S. Naka, "Preparation of Compounds in BaO–$TiO_2$ System by Corprecipitation of Metal Alkoxides," *Funtai Oyobi Fummatsuyakin*, **25** [5] 20–3 (1978).
[3]E. P. Turevskaya, N. Ya.Turova, and A. V. Novoselova, "Investigation of the Formation of Bimetallic Alkoxides, Reaction of Barium Ethoxide and Titanium Ethoxide," *Dok. Akad. Nauk SSSR*, **242** [4] 883–6 (1978).
[4]R. E. Riman, "The Role of the Chemical Processing Variables for the Synthesis of Ideal SrTiO3 Powder," Ph.D. Thesis, Department of Materials Science and Engineering, MIT, Cambridge, MA, 1987.

[5]R. H. II Heistand, Y. Oguri, H. Okamura, W. C. Moffat, B. Novich, E. A. Barringer, and H. K. Bowen, "Synthesis and Processing of Submicrometer Ceramic Powders, in Science of Ceramic Chemical Processing"; pp. 482–96 in Edited by L. L. Hench, and D. R. Ulhmann. John Willey and Sons, New York, 1986.

[6]D. Payne, D. J. Eichorst, L. F. Francis, and J.-F. Campion, "Molecular Precursors for the Chemical Processing of Advanced Electrical Ceramics"; pp. 499–512 in *Chemical Processing of Ceramics*, Edited by L. L. Hench, and J. K. West. John Wiley and Sons, 1992.

[7]G. A. Hebbink, D. N. Reinboudt, and F. C. J. M. van Veggel, "Increased Luminescent Lifetimes of $Ln^{3+}$ Complexes Emitting in the Near-Infrared as a Result of Deuteration," *Eur. J. Org. Chem*., 4101–6 (2001).

[8]L. H. Sloof and A. Polman, "Optical Properties of Erbium-Doped Organic Polydentate Cage Complexes," *J. App. Phys*., **83**, 497–503 (1998).

[9]M. P. O. Wolbers, F. C. J. M. van Veggel, B. H. M. Snellink-Ruel, J. W. Hofstraat, F. A. J. Geurts, and D. N. Reinhoudt, "Novel Preorganized Hemispherands to Encapsulate Rare Earth Ions: Shielding and Ligand Deuteration for Prolonged Lifetimes of Excited $Eu^{3+}$ Ions," *J. Amer. Chem. Soc*., **119**, 138–44 (1997).

[10]M. P. O. Wolbers, F. C. J. M. van Veggel, F. G. A. Peters, E. S. E. van Beelen, J. W. Hofstraat, F. A. J. Geurts, and D. N. Reinhoudt, "Sensitized Near-Infrared Emission from $Nd^{3+}$ and $Er^{3+}$ Complexes of Fluorescein-Bearing Calix[4]Arene Cages," *Chem. Eur. J*., **4**, 772–80 (1998).

[11]Y. Hasegawa, T. Okhubo, K. Sogabe, Y. Kawamura, Y. Wada, N. Nakashima, and S Yanagida, "Luminescence of Novel Neodymium Sulfonylaminate Complexes in Organic Media," *Angew. Chem. Int. Ed*., **39**, 357–60 (2000).

[12]D. Smith, S. Chen, S. Kumar, J. Ballato, C. Topping, and S. Foulger, "Perfluorocyclobutyl Copolymers for Microphotonics," *Adv. Mater*., **14**, 1585–9 (2002).

[13]A. Kornienko, T. Emge, G. A. Kumar, R. E. Riman, and J. G. Brennan, "Lanthanide Clusters with Internal Ln: Highly Emissive Molecules with Solid State Cores," *J. Amer. Chem. Soc*., **127**, 3501–5 (2005).

[14]S. Banerjee, L. Huebner, M. D. Romanelli, G. A. Kumar, R. E. Riman, T. J. Emge, and J. G. Brennan, "Oxoselenido Clusters of the Lanthanides: Rational Introduction of Oxo Ligands and Near-IR Emission from Nd(III)," *J. Am. Chem. Soc*., **127**, 15900–6 (2005).

[15]A. Kornienko, S. Banerjee, G. A. Kumar, R. E. Riman, T. Emge, and J. Brennan, "Heterometallic Lanthanide Main Group Metal Chalcogenido Clusters; Highly Emissive Precursors to Ternary Solid State Materials," *J. Am. Chem. Soc*., **127**, 14008–14 (2005).

[16]L. Huebner, A. Kornienko, T. J. Emge, and J. G. Brennan, "Lanthanide Clusters with Internal Ln: Fragmentation and the Formation of Dimers with Bridging $Se^{2-}$ and $SeSe^{2-}$ Ligands," *Inorg. Chem*., **44**, 5118–22 (2005).

[17]A. Kornienko, L. Huebner, D. Freedman, T. Emge, and J. Brennan, "Lanthanide-Transition Metal Chalcogenido Cluster Materials," *Inorg. Chem*., **42**, 8476–80 (2003).

[18]M. Fitzgerald, T. Emge, and J. Brennan, "Chalcogen Rich Lanthanide Clusters with Fluorinated Thiolate Ligands," *Inorg. Chem*., **41**, 3528–33 (2002).

[19]D. Freedman, T. Emge, and J. Brennan, "Chalcogen Rich Clusters of the Lanthanides with $Te^{2-}$, $(TeTe)^{2-}$, TePh, TeTePh, $(TeTeTe(Ph)TeTe)^{5-}$ and $[(TeTe)4TePh]^{9-}$ ligands," *Inorg. Chem*., **41**, 492–500 (2002).

[20]A. Kornienko, T. Emge, G. Hall, and J. Brennan, "Chalcogen Rich Clusters of the Lanthanides from Halogenated Starting Materials (II): Selenido Compounds and the Synthesis of $LnSe_x$," *org. Chem*., **41**, 121–6 (2002).

[21]A. Kornienko, T. Emge, and J. Brennan, "Chalcogen Rich Lanthanide Clusters: Cluster Reactivity the Control of Structure by Ancillary Ligands," *J. Am. Chem. Soc*., **123**, 11933–9 (2001).

[22]D. Freedman, S. Sayan, M. Croft, T. Emge, and J. Brennan, "Heterovalent Clusters: $Ln_4Se(SePh)_4$ ($Ln_4 = Sm_4$, $Y_4b_4$, $Sm_2Yb_2$, $Nd_2Yb_2$)," *J. Am. Chem. Soc*., **121**, 11713–9 (1999).

[23]J. Melman, M. Fitzgerald, D. Freedman, T. Emge, and J. Brennan, "Chalcogen Rich Lanthanide Clusters from Lanthanide Halide Starting Materials; a New Approach to the Low Temperature Synthesis of $LnS_x$ Solids from Molecular Precursors," *J. Am. Chem. Soc*., **121**, 10247–8 (1999).

[24]D. Freedman, T. Emge, and J. Brennan, "$(THF)_8Ln_8E_6(EPh)_{12}$ Cluster Reactivity: Systematic Control of Ln, E, EPh, and Neutral Donor Ligands," *Inorg. Chem*., **38**, 4400–4 (1999).

[25]J. Melman, T. Emge, and J. Brennan, "Cubic Lanthanide Sulfido Clusters: Synthesis, Structure, and Coordination Chemistry," *Inorg. Chem*., **38**, 2117–22 (1999).

[26]D. Freedman, J. Melman, T. Emge, and J. Brennan, "Cubane Clusters Containing Lanthanide Ions: $(py)_2Yb_4Se_4(SePh)_4$ and $(py)_{10}Yb_6S_6(SPh)_6$," *Inorg. Chem*., **37**, 4162–3 (1998).

[27]J. Melman, T. J. Emge, and J. Brennan, "Cubic Lanthanide Sulfido Clusters: $Ln_8S_6(SPh)_{12}(THF)_8$ (Ln = Pr, Nd, Gd)," *Chem. Commun*., 2269–70 (1997).

[28]D. Freedman, T. J. Emge, and J. G. Brennan, "Unexpected Routes to Lanthanide Chalcogenide Clusters: $Sm_8Se_6(SePh)_{12}(THF)_8$ and $[Sm_7S_7(SePh)_6(DME)_7]$," *J. Am. Chem. Soc*., **119**, 11112–3 (1997).

[29]M. Munzar, C. Koughia, D. Tonchev, K. Maeda, T. Ikari, C. Haugen, R. Decorby, J. N. McMullin, and S. O. Kasap, "Optical Properties of Er-Doped $Ga_x(Ge_{0.3}Se_{0.7})_{100x}$ Glasses," *Opt. Mater*., **28** [3] 225–30 (2006).

[30]A. J. Silversmith, W. Lenth, and R. M. Macfarlane, "Green Infrared-Pumped Erbium Upconversion Laser," *Appl. Phys. Lett*., **51**, 1977–9 (1987).

[31]G. S. Maciel, C. B. de Arajuo, Y. Messaddeq, and M. A. Aegerter, "Frequency Upconversion in $Er^{3+}$-Doped Fluoroindate Glasses Pumped at 1.48 μm," *Phys. Rev. B*, **55**, 6335–42 (1997).

[32]T. Hebert, R. Wannermacher, W. Lenth, and R. M. MacFarlane, "Blue and Green cw Upconversion Lasing in Er: $YLiF_4$," *Appl. Phys. Lett*., **57**, 1727–9 (1990).

[33]E. Downing, L. Hesselink, J. Ralston, and R. M. Macfarlane, "A Three-Color, Solid-State, Three-Dimensional Display," *Science*, **273**, 1185–7 (1986).

[34]R. N. Bhargava, D. Gallaghar, X. Hong, and A. Nurmikko, "Optical Properties of Manganese-Doped Nanocrystals of Zinc Sulfide," *Phys. Rev. Lett*., **72** [3] 416–9 (1994).

[35]K. Soga, W. Wang, R. E. Riman, J. B. Brown, and K. R. Mikeska, "Luminescent Properties of Nanostructured $Dy^{3+}$- and $Tm^{3+}$-Doped Lanthanum Chloride Prepared by Reactive Atmosphere Processing of Sol–Gel Derived Lanthanum Hydroxide," *J. Appl. Phys*., **93** [5] 2946–51 (2003).

[36]P. C. Becker, N. A. Olsson, and J. R. Simpson, *Erbium Doped Fiber Amplifiers—Fundamental and Technology*. Academic Press, NY, 1999.

[37]J. Fick, E. J. Knystautas, A. Villeneuve, A. Schiettekatte, S. Roorda, and K. A. Richardson, "High Photoluminescence in Erbium-Doped Chalcogenide Thin Films," *J. Non-Cryst. Solids*, **272**, 200–8 (2000).

[38]C. C. Ye, D. W. Hewak, M. Hempstead, M. Samson, and D. N. Payne, "Spectral Properties of $Er^{3+}$-Doped Gallium Lanthanum Sulphide Glass," *J. Non-Cryst. Solids*, **208**, 56–63 (1996).

[39]G. A. Kumar, R. E. Riman, Elias Snitzer, and J. Ballato, "Solution Synthesis and Spectroscopic Characterization of High $Er^{3+}$ Content $LaF_3$ for Broadband 1.5 μm Amplification," *J. Appl. Phys*., **95**, 40–7 (2004).

[40]G. A. Kumar, R. E. Riman, S. C. Chae, Y. N. Jang, I. K. Bae, and H. S. Moon, "Synthesis and Spectroscopic Characterization of $CaF_2$: $Er^{3+}$ Single Crystal for Highly Efficient 1.53 μm Amplification," *J. Appl. Phys*., **95**, 3243–9 (2004).

[41]T. Forster, "Intermolecular Energy Transference and Fluorescence," *Ann. Phys*., **2**, 55–9 (1948).

[42]D. L. Dexter, "A Theory of Sensitized Luminescence in Solids," *J. Chem. Phys*., **21**, 836–50 (1953).

[43]G. A. Kumar, R. E. Riman, S. Banerjee, A Kornienko, and J. G. Brennan, "Chalcogenide-Bound Erbium Complexes: Paradigm Molecules for Infrared Fluorescence Emission," *Chem. Mat*., **17**, 5130–5 (2005).

[44]M. J. F. Diggonet, *Rare Earth Doped Fiber Lasers and Amplifiers*, 2nd edition, p. 449 Marcel Dekker Inc., New York, 1993.

[45]L. H. Slooff, A. Polman, S. I. Klink, G. A. Hebbink, L. Grave, F. C. J. M. van Veggel, D. N. Reinhoudt, and J. W. Hofstraat, "Optical Properties of Lissamine Functionalized $Nd^{3+}$ Complexes in Polymer Waveguides and Solution," *Opt. Mater*., **14**, 101–7 (2000).

[46]M. P. O. Wolbers, F. C. J. M. van Veggel, J. W. Hofstraat, F. A. J. Geurts, and D. N. Reinhoudt, "Luminescence Properties of M-Terphenyl-Based $Eu^{3+}$ and $Nd^{3+}$ Complexes: Visible and Near-Infrared Emission," *J. Chem. Soc. Perkin Trans*., **11**, 2275–82 (1997).

[47]M. P. O. Wolbers, F. C. J. M. van Veggel, B. H. M. Snellink-Ruel, J. W. Hofstraat, F. A. J. Geurts, and D. N. Reinhoudt, "Photophysical Studies of M-Terphenyl-Sensitized Visible and Near-Infrared Emission from Organic 1: 1 Lanthanide Ion Complexes in Methanol Solutions," *J. Chem. Soc. Perkin Trans*., **10**, 2141–50 (1998).

[48]S. I. Klink, G. A. Hebbink, L. Grave, F. C. J. M. van Veggel, D. N. Reinhoudt, L. H. Slooff, A. Polman, and J. W. Hofstraat, "Sensitized Near-Infrared Luminescence from Polydentate Triphenylene-Functionalized $Nd^{3+}$, $Yb^{3+}$, and $Er^{3+}$ Complexes," *J. Appl. Phys*., **86**, 1181–5 (1999).

[49]Y. Wada, T. Okubo, M. Ryo, T. Nakazawa, Y. Hasegawa, and S. Yanagida, "High Efficiency Near-IR Emission of Nd(III) Based on Low-Vibrational Environment in Cages of Nanosized Zeolites," *J. Am. Chem. Soc*., **122**, 8583–4 (2000).

[50]G. A. Kumar, J. Lu, A. A. Kaminskii, and K. Ueda, "Spectroscopic and Stimulated Emission Characteristics of $Nd^{3+}$ in Transparent YAG Ceramics," *IEEE J. Quant. Elect*., **40** [6] 747–58 (2004).

[51]G. A. Kumar *et al*., "Infrared Fluorescence and Optical Gain Characteristics of Chalcogenide-bound Erbium Cluster-Fluoropolymer Nanocomposites," *Appl. Phys. Lett*., **88**, 091902 (2006).

[52]T. Kobayashi, S. Nakatsuka, T. Iwafuji, K. Kuriki, N. Imai, T. Nakamoto, C. D. Claude, K. Sasaki, Y. Koike, and Y. Okamoto, "Fabrication and Superfluorescence of Rare-Earth Chelate-Doped Graded Index Polymer Optical Fibers," *Appl. Phys. Lett*., **71**, 2421–3 (1997).

[53]G. Nykolak, M. Haner, P. C. Becker, J. Schmulovich, and Y. H. Wong, "Concentration-Dependent $^4I_{13/2}$ Lifetimes in $Er^{3+}$-Doped Fibers and $Er^{3+}$-Doped Planar Waveguides," *IEEE Photonic. Tech. Lett*., **5**, 1014–6 (1993).

[54]G. A. Kumar, C. W. Chen, R. E. Riman, S. Chen, D. Smith, and J. Ballato, "Optical Properties of $CaF_2$: Er/6F Polymer Composite Wave-Guide," *Appl. Phys. Lett*, **86**, 241105 (2005). □